

Polarimetric Method of Determining Magnetic Fields in Accretion Discs around Black Holes

**Gnedin Yu.N., Silant'ev N.A., Piotrovich M.Yu.,
Natsvlishvili T.M., Buliga S.D.**

Central Astronomical Observatory at Pulkovo, Saint-Petersburg

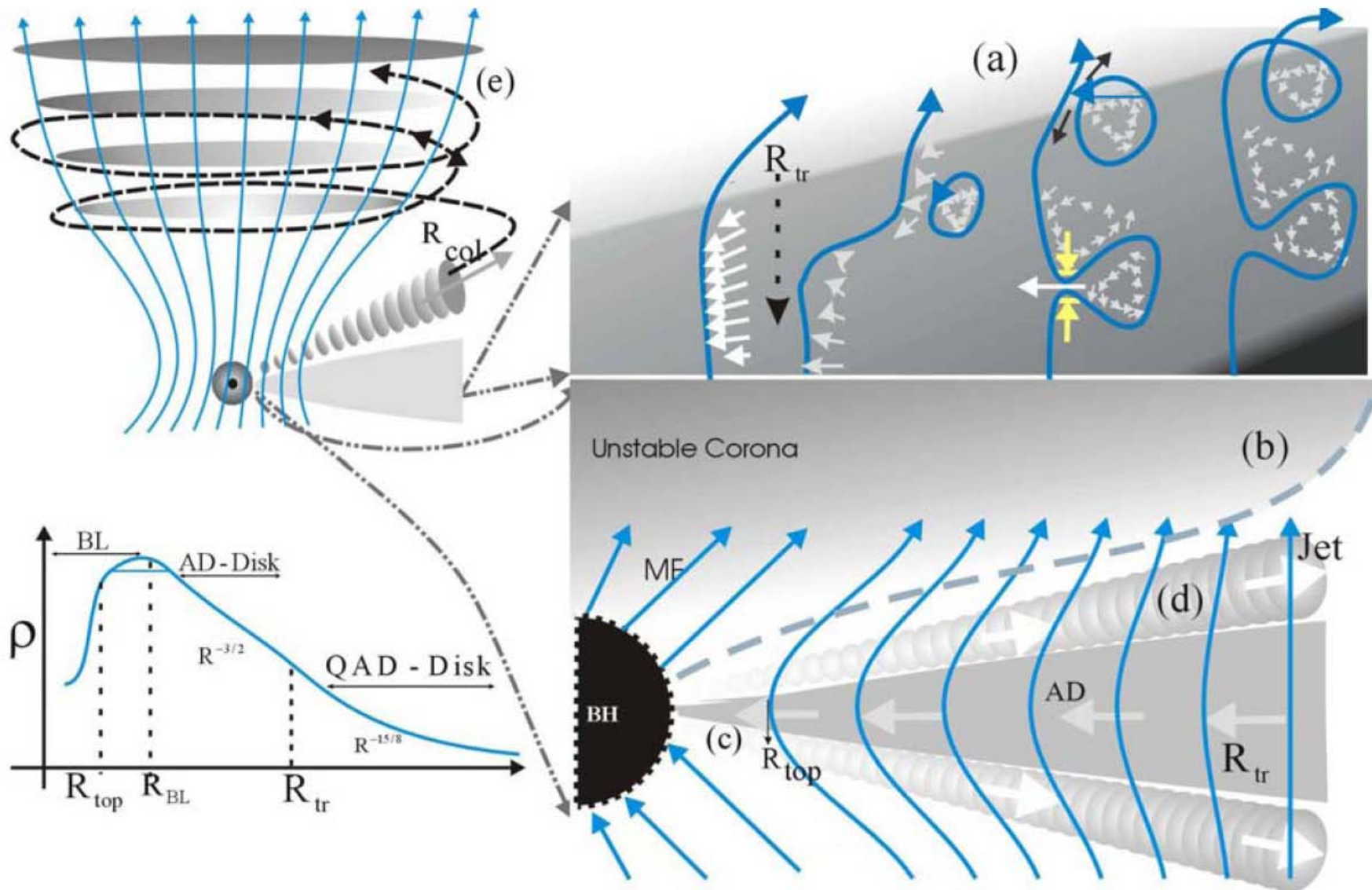
Abstract

We present the review of basic methods of measurements of magnetic fields with application to accreting supermassive black holes. The problem of the connection between jet and accretion disk is discussed. The results of polarimetric radio and optical observations of QSOs and AGNs are presented in this talk.

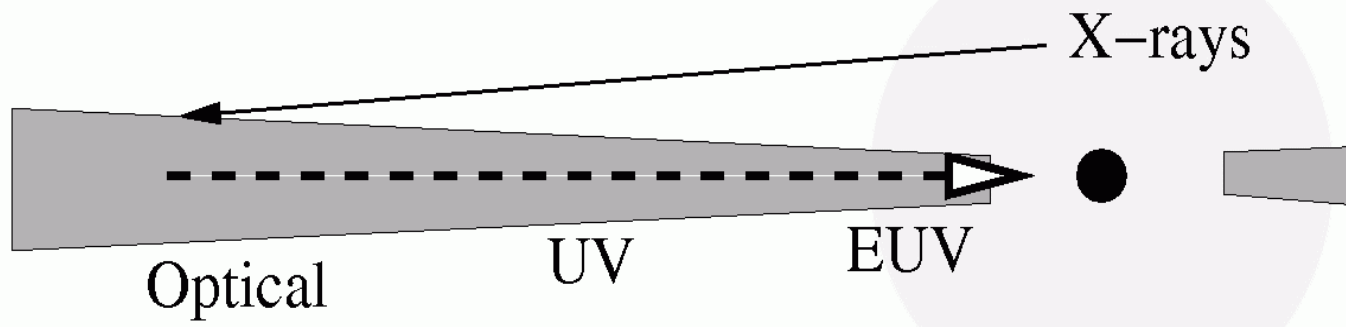
Table 1 Characteristic scales in the nuclear regions in active galaxies

| | l [R_g] | l_8 [pc] | θ_{Gpc} [mas] | τ_c [yr] | τ_{orb} [yr] |
|----------------------------------|------------------|-----------------------|--------------------------------|------------------|-----------------------------|
| Event horizon: | 1–2 | 10^{-5} | 5×10^{-6} | 0.0001 | 0.001 |
| Ergosphere: | 1–2 | 10^{-5} | 5×10^{-6} | 0.0001 | 0.001 |
| Corona: | 10^1 – 10^2 | 10^{-4} – 10^{-3} | 5×10^{-4} | 0.001–0.01 | 0.2–0.5 |
| Accretion disk: | 10^1 – 10^3 | 10^{-4} – 10^{-2} | 0.005 | 0.001–0.1 | 0.2–15 |
| Jet formation: | $>10^2$ | $>10^{-3}$ | $>5 \times 10^{-4}$ | >0.01 | >0.5 |
| Jet visible in the radio: | $>10^3$ | $>10^{-2}$ | >0.005 | >0.1 | >15 |
| Broad line region: | 10^2 – 10^5 | 10^{-3} –1 | 0.05 | 0.01–10 | 0.5–15000 |
| Molecular torus: | $>10^5$ | >1 | >0.5 | >10 | >15000 |
| Narrow line region: | $>10^6$ | >10 | >5 | >100 | >500000 |

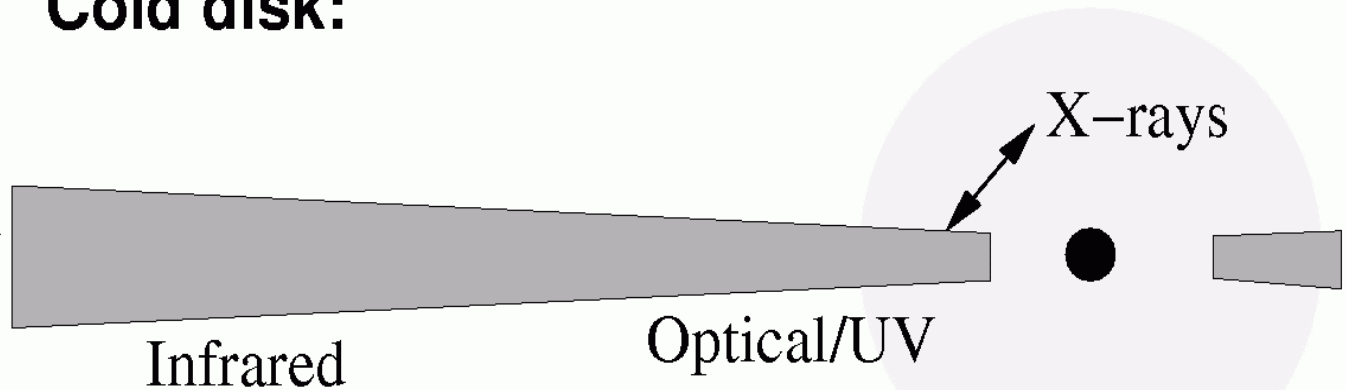
Column designation: l – dimensionless scale in units of the gravitational radius, GM/c^2 ; l_8 – corresponding linear scale, for a black hole with a mass of $5 \times 10^8 M_\odot$; θ_{Gpc} – corresponding largest angular scale at 1 Gpc distance; τ_c – rest frame light crossing time; τ_{orb} – rest frame orbital period, for a circular Keplerian orbit. Adapted from (Lobanov & Zensus 2006)



Hot disk:

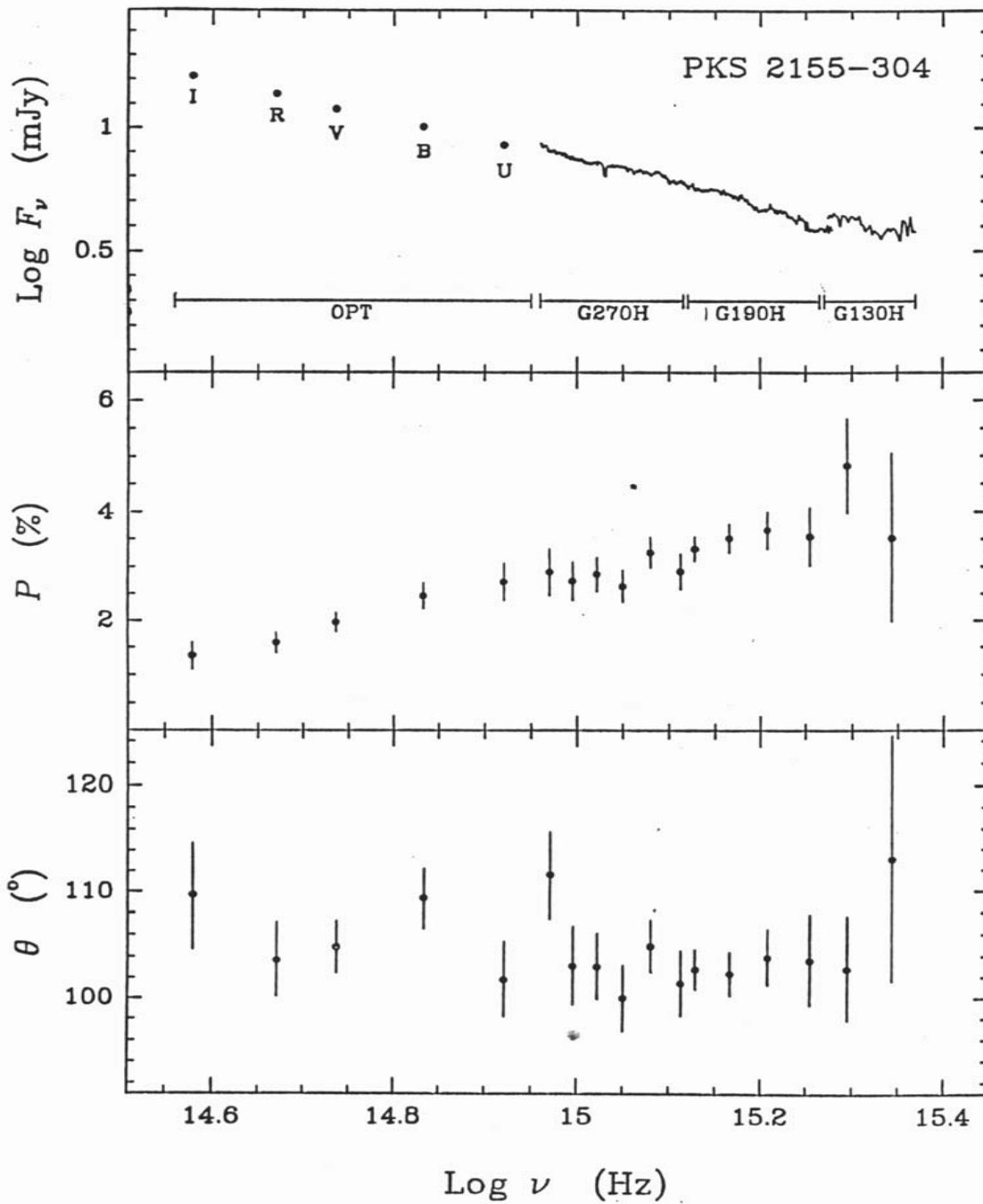


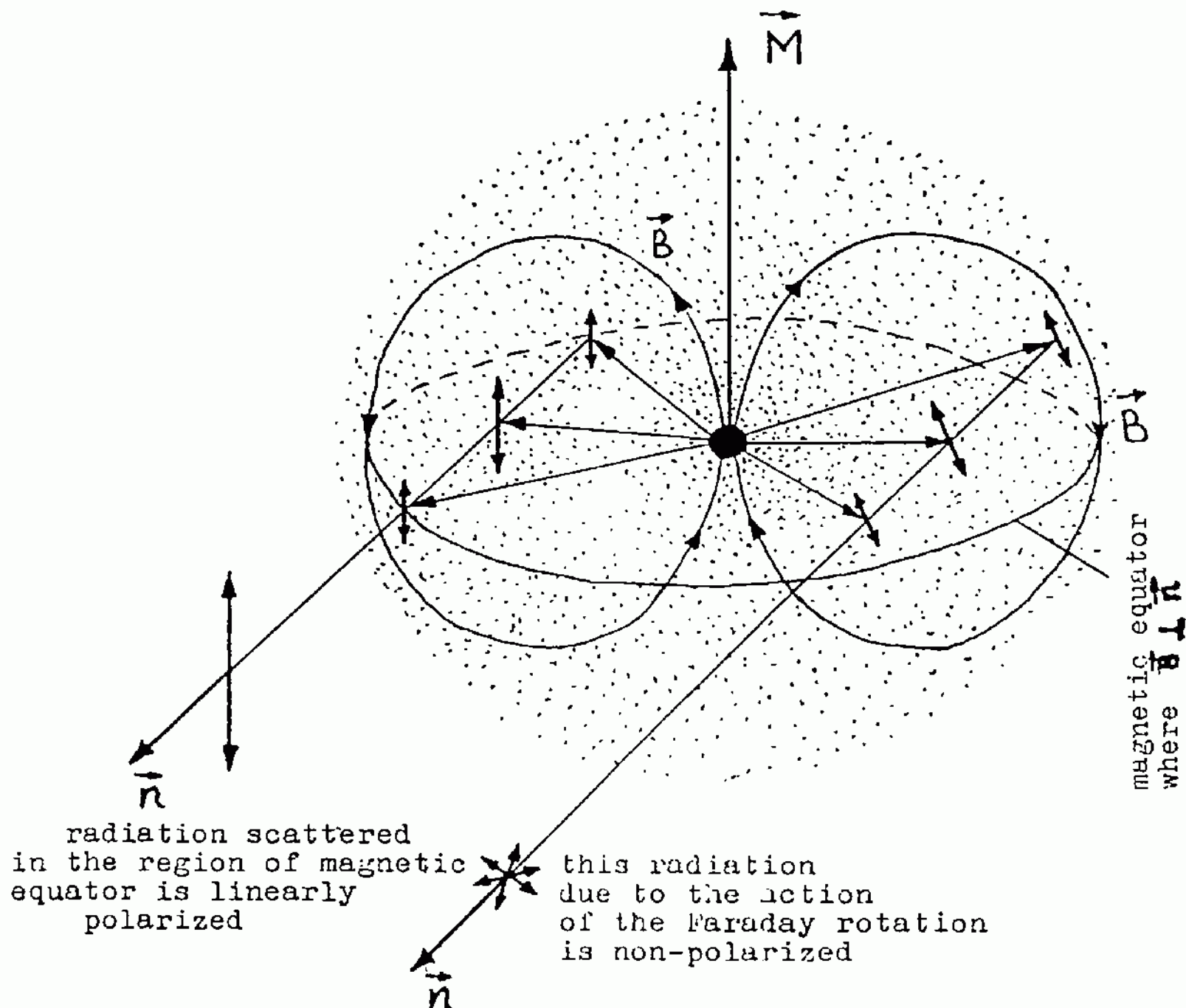
Cold disk:

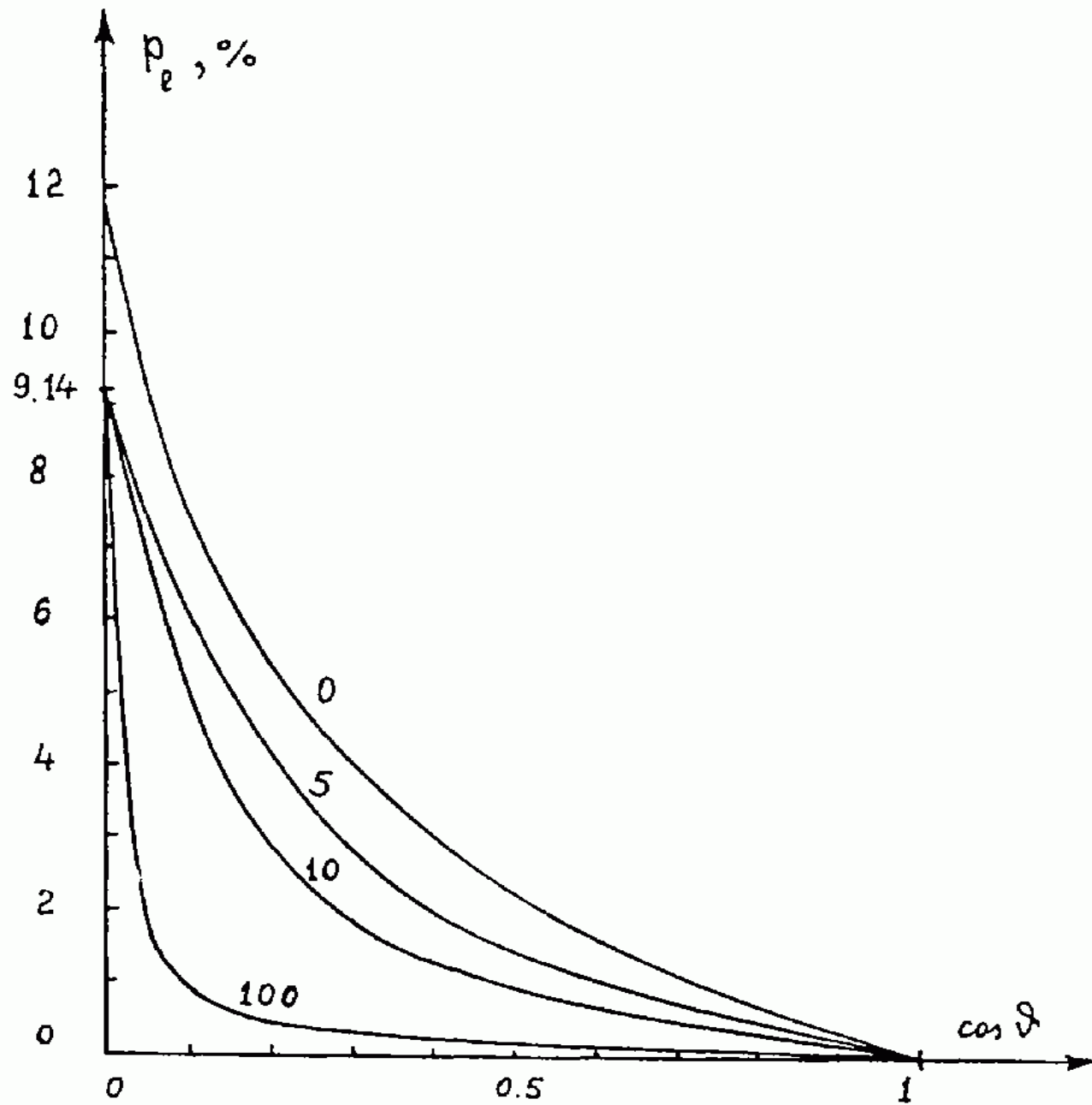


**BH
mass**

Mdot







Three basic regions of Magnetic Fields:

(a) Accretion Disk

(b) Relativistic Jet

(c) Accretion Disk Wind and Outflow

$$P_l(\vec{B}, \vec{n}) = \frac{P_l(0, \mu)}{\sqrt{1 + \delta^2 \cos^2 \theta}} ; \quad \tan 2\chi = \delta \cos \theta$$

$$\delta = 0.8 \lambda_{rest}^2 (\mu m) B - \text{depolarization parameter}$$

For an accretion disk: $\delta = \delta_{\perp} \sqrt{1 - \mu^2} + \delta_{\parallel} \mu ; \quad \mu = \cos i$

$$\delta_{\perp} = 0.8 \lambda_{rest}^2 (\mu m) B_{\perp} , \quad \delta_{\parallel} = 0.8 \lambda_{rest}^2 (\mu m) B_{\parallel}$$

$$B_{\perp}(R) = B_H \left(\frac{R_H}{R} \right)^n , \quad n = \frac{5}{4} - \text{Pariev et al., 2003.}$$

$$B_{\parallel} = B_j = B_{\perp} \left(\frac{L_j}{L_d} \frac{H}{R} \right)^{1/2} \approx B_{\perp} \frac{L_j}{L_d}$$

Magnetic Equipartition

R.-Y. Ma, F. Yuan, arXiv:0706.0124.

$$B_H = k \sqrt{2 L_{bol} / \epsilon c} / R_H, \quad k \approx 1$$

$$L_{bol} = \epsilon \dot{M} c^2, \quad R_H = \frac{GM}{c^2} \left(1 + \sqrt{1 - \left(\frac{a}{M} \right)^2} \right)$$

| a/M | ϵ_M | Spin Equilibrium? | Characterization |
|-------|--------------|-------------------|--------------------------------------|
| 0.0 | 0.057 | no | standard thin disk; nonspinning BH |
| 0.95 | 0.19 | yes | turbulent MHD disk |
| 0.998 | 0.32 | yes | standard thin disk; photon recapture |
| 1.0 | 0.42 | yes | standard thin disk; max spin BH |

$$B_{Ed} = 6.2 \times 10^8 \left(\frac{M_\odot}{M_{BH}} \right)^{1/2} \left(\frac{\eta}{\epsilon} \right)^{1/2} \frac{1}{1 + \sqrt{1 - \left(\frac{a}{M} \right)^2}}, \quad \eta = \frac{L_{bol}}{L_{Ed}}$$

Magnetic Field of QSOs in the Epoch of Reionization

| QSO | z | $L_{\text{bol}}/L_{\text{Ed}}$ | $a/M = 0,$ $\varepsilon = 0.057$ | $a/M = 0.95,$ $\varepsilon = 0.19$ | $a/M = 0.998,$ $\varepsilon = 0.32$ | $a/M = 1.0,$ $\varepsilon = 0.42$ |
|------------|-------|--------------------------------|-------------------------------------|---------------------------------------|--|--------------------------------------|
| J0836+0054 | 5.810 | 0.44 | 9.0×10^3 G | 7.5×10^3 G | 7.15×10^3 G | 6.6×10^3 G |
| J1030+0524 | 6.309 | 0.50 | 1.5×10^4 G | 1.22×10^4 G | 1.16×10^4 G | 1.0×10^4 G |
| J1044-0125 | 5.778 | 0.31 | 7.1×10^3 G | 6.0×10^3 G | 5.7×10^3 G | 5.3×10^3 G |
| J1306+0356 | 6.016 | 0.61 | 1.8×10^4 G | 1.5×10^4 G | 1.43×10^4 G | 1.4×10^4 G |
| J1411+1217 | 5.927 | 0.94 | 3.5×10^4 G | 2.93×10^4 G | 2.8×10^4 G | 2.7×10^4 G |
| J1623+312 | 6.247 | 1.11 | 3.5×10^4 G | 2.93×10^4 G | 2.8×10^4 G | 2.7×10^4 G |

The Magnetic Flux Conservation in Accretion Disk:

$$a \sim \frac{1}{\lambda^{2/3}}, b \sim \lambda^{2/3}, B_z \sim R_\lambda^{-2}, B_\perp \sim R_\lambda^{-1}$$

$$\lambda_{res} \rightarrow a = b, \lambda_{res} = f(M_{BH}, L_{bol} / L_{Edd}, a_*)$$

$a_* = 0$ - Schwarzschild BH, $a_* = 1$ - Kerr BH.

$$P_{rel} = \frac{P_l(B, \mu)}{P_l(0, \mu)}$$

$$a = b = 4, P_{rel} = 0.3522, \chi = 20^\circ.7$$

$$a = 8, b = 2, P_{rel} = 0.1279, \chi = 41^\circ.2$$

$$a = 2, b = 8, P_{rel} = 0.1279, \chi = 0^\circ.9$$

Estimation of Magnetic Field Strength at the Event Horizon of SMBH by Optical Polarization in Continuum.

NGC 4258: $i = 83^\circ \pm 4^\circ$

$$P_l(\lambda\lambda 4000 - 4800\text{\AA}) = (0.38 \pm 0.03)\%, \chi = 12^\circ \pm 2^\circ$$

$$P_l(\lambda\lambda 5100 - 6100\text{\AA}) = (0.35 \pm 0.01)\%, \chi = 7^\circ \pm 1^\circ$$

$$P_l(\lambda\lambda 7500 - 8000\text{\AA}) = (0.29 \pm 0.02)\%, \chi = 8^\circ \pm 2^\circ$$

The classical result (Chandrasekhar-Sobolev Theory):

$$P_l = 6.9\% (\mu = \cos i = 0.122)$$

$$R_\lambda = 0.95 \times 10^{10} \left(\frac{\lambda_{rest}}{\mu m} \right)^{4/3} \left(\frac{M_{BH}}{M_\odot} \right)^{2/3} \left(\frac{L_{bol}}{\varepsilon L_{Edd}} \right)^{1/3} \quad (\text{Poindexter et al., 2007})$$

The faraday Depolarization Factor: $\delta = 0.8 \lambda_{rest}^2 B(R_\lambda)$

$$B_H = B(R_\lambda) \left(\frac{R_\lambda}{R_H} \right)^n, \quad n = \frac{5}{4} \text{ - the standard Shakura-Sunyaev Disk}$$

$$B_H = 2.5 \times 10^4 G$$

NGC 4258

Zeeman Spectropolarimetry 18cm OH Megamaser Emission
(Modjaz et al., 2005)

1σ upper limit: 30mG at 0.14pc.

$$B_H = 2.5 \times 10^4 G, n = \frac{5}{4}$$

$$B_{mas}(0.14 pc) = 20mG \text{ for } \frac{a}{M_{BH}} \approx 1$$

NGC 3516 (Smith et al., 2002)

$$M_{BH} = 10^{7.36} M_{\odot}, L_{bol} = 10^{44.9} \text{ erg/s}, i = 38^{\circ}.3$$

$$P_l(\lambda\lambda 6500 - 6740 \text{ \AA}) = (0.15 \pm 0.04)\%, \chi = 30^{\circ}.1 \pm 8^{\circ}$$

$$P_l(\text{theory}) = 0.83\% ; B_H = 10^4 G (\varepsilon = 0.32, a_* = 0.998)$$

$$a_* = a/M_{BH} - \text{Kerr parameter.}$$

NGC 4151

$$M_{BH} = (1.53_{-0.89}^{+1.06}) M_{\odot}, L_{bol} = 10^{43.73} \text{ erg/s}, i = 60^{\circ}$$

$$P_l(\lambda\lambda 3800 - 5300 \text{ \AA}) = 0.26\%, P_l(\text{theory}) = 2.257\%$$

$$(\text{Chandrasekhar, 1950}) B_H = 1.5 \times 10^4 G, \varepsilon = 0.32$$

NGC 5548

$$M_{BH} = 10^{8.05} M_{\odot}, L_{bol} = 10^{44.83} \text{ erg/s}, i = 45^{\circ}$$

The classical Thomson limit: $P_l = 1.115\%$

$$P_l(\lambda\lambda 6520 - 6860 \text{ \AA}) = (0.69 \pm 0.01)\%, B_H = 720 G, \varepsilon = 0.32$$

| Model | $B_{eq}(R)$ | $P_l(\lambda)$ | Refs. |
|--|-------------------|-----------------------|------------------------|
| Accretion disk with ion supported flows. | $\sim R^{-5/4}$ | $\sim \lambda^{-1/3}$ | Begelman, 1988 |
| Sunayev-Shakura disk Region (a), $P_r \gg P_g$ | $\sim R^{-3/4}$ | $\sim \lambda^{-1}$ | Shakura-Sunayev, 1973 |
| Shakura-Sunayev disk (b) $P_g \gg P_r$ | $\sim R^{-9/8}$ | $\sim \lambda^{-1/2}$ | Shakura-Sunayev, 1973 |
| Shakura-Sunayev disk (c) $P_g \gg P_r$ | $\sim R^{-21/16}$ | $\sim \lambda^{-1/4}$ | Shakura-Sunayev, 1973 |
| Hot Accretion Disk with Plasma Viscosity | $\sim R^{-15/28}$ | $\sim \lambda^{-9/7}$ | Kafatos, 1988 |
| Payne-Eardley Disk $P = P_g, \alpha = 1$ | $\sim R^{-21/8}$ | $\sim \lambda^{-1/8}$ | Shapiro-Teukolsky |
| Magnetic Accretion-Jet Ejection Disk without equipartition | $\sim R^{-5/2}$ | $\sim \lambda^{4/3}$ | Case and Keppens, 2002 |
| Accretion disk with non-zero torque on its inner edge | $\sim R^{-15/16}$ | $\sim \lambda^{-1}$ | Agol, Krolik, 2000 |
| Disk with reprocessing | $\sim R^{-7/4}$ | $\sim \lambda^{-1/8}$ | |

Магнитный диск: $B^2/8\pi = \alpha \sqrt{P_{gas} P_{rod}}, P_l \sim \lambda^{-15/16}$.

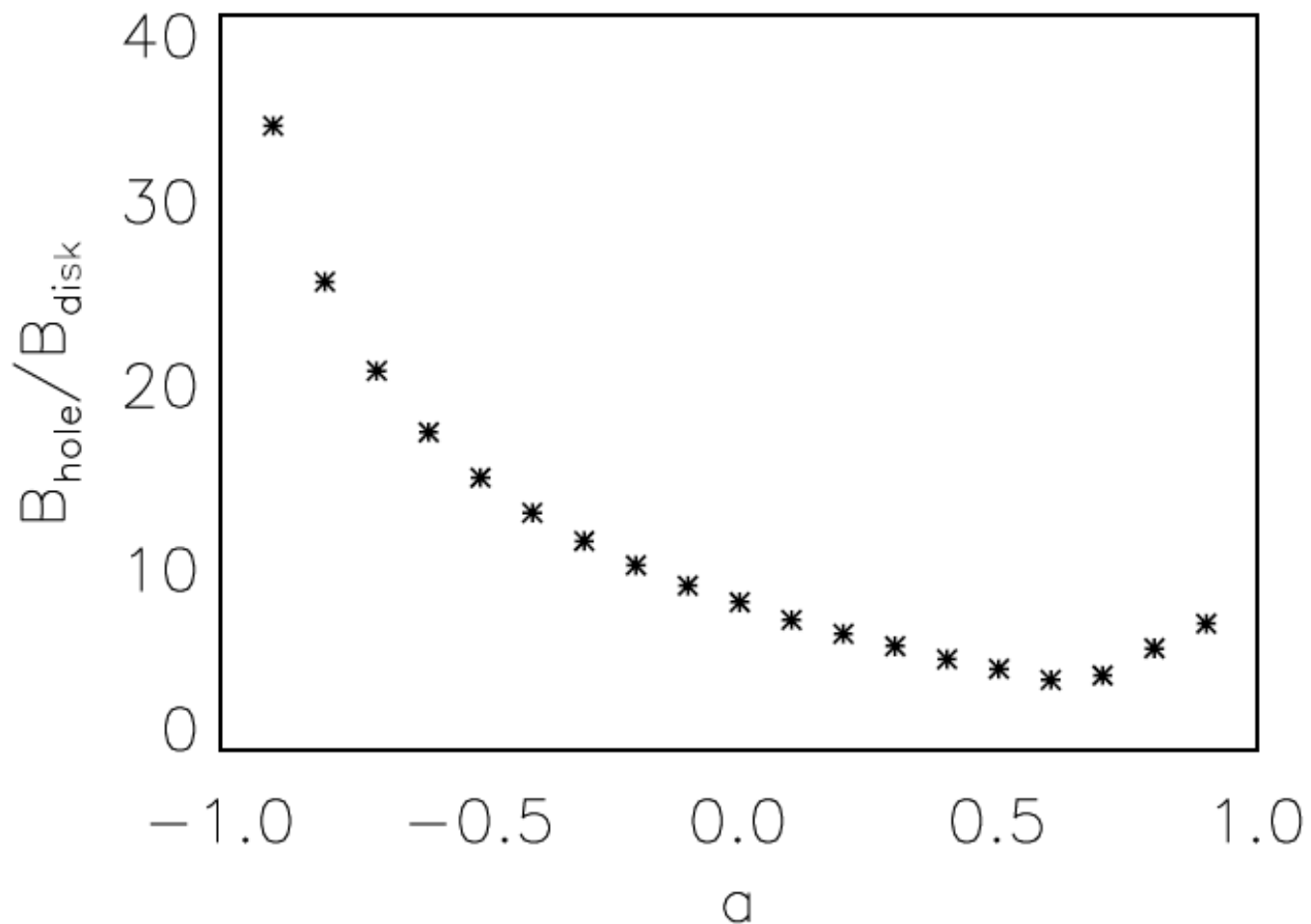


Figure 7. Ratio of horizon-threading magnetic field as measured by ZAMO observers and magnetic field strength in the accretion disk as a function of spin.

(D. Garofalo, *The Astrophysical Journal*, 699:400–408, 2009 July 1)

Table 2. New circular polarization measurements of quasars

| Object | z | p_{lin} (%) | θ_{lin} ($^{\circ}$) | p_{circ} (%) |
|-----------|-------|----------------------|--------------------------------------|-----------------------|
| 1120+019 | 1.465 | 1.95 ± 0.27 | 9 ± 4^c | -0.02 ± 0.05 |
| 1124-186 | 1.048 | 11.68 ± 0.36 | 37 ± 1^g | -0.04 ± 0.08 |
| 1127-145 | 1.187 | 1.30 ± 0.40 [w] | 23 ± 10^a | -0.05 ± 0.05 |
| 1157+014 | 1.990 | 0.76 ± 0.18 | 39 ± 7^f | -0.10 ± 0.08 |
| 1205+146 | 1.640 | 0.83 ± 0.18 | 161 ± 6^f | -0.10 ± 0.09 |
| 1212+147 | 1.621 | 1.45 ± 0.30 | 24 ± 6^c | 0.15 ± 0.09 |
| 1215-002* | 0.420 | 23.94 ± 0.70 | 91 ± 1^g | -0.42 ± 0.40 |
| 1216-010 | 0.415 | 11.20 ± 0.17 | 100 ± 1^g | -0.01 ± 0.07 |
| 1222+228 | 2.058 | 0.92 ± 0.14 | 169 ± 4^g | 0.01 ± 0.10 |
| 1244-255 | 0.633 | 8.40 ± 0.20 [w] | 110 ± 1^a | -0.23 ± 0.20 |
| 1246-057 | 2.236 | 1.96 ± 0.18 [w] | 149 ± 3^e | 0.01 ± 0.03 |
| 1254+047 | 1.024 | 1.22 ± 0.15 [w] | 165 ± 3^b | -0.02 ± 0.04 |
| 1256-229* | 0.481 | 22.32 ± 0.15 | 157 ± 1^g | 0.18 ± 0.04 |
| 1309-056 | 2.212 | 0.78 ± 0.28 | 179 ± 11^c | -0.08 ± 0.06 |
| 1331-011 | 1.867 | 1.88 ± 0.31 | 29 ± 5^c | -0.04 ± 0.06 |
| 1339-180 | 2.210 | 0.83 ± 0.15 | 20 ± 5^g | -0.01 ± 0.07 |
| 1416-129 | 0.129 | 1.63 ± 0.15 [w] | 44 ± 3^b | 0.05 ± 0.06 |
| 1429-008 | 2.084 | 1.00 ± 0.29 | 9 ± 9^c | 0.02 ± 0.08 |
| 2121+050 | 1.878 | 10.70 ± 2.90 [w] | 68 ± 6^a | 0.02 ± 0.15 |
| 2128-123 | 0.501 | 1.90 ± 0.40 [w] | 64 ± 6^d | -0.04 ± 0.03 |
| 2155-152 | 0.672 | 22.60 ± 1.10 [w] | 7 ± 2^a | -0.35 ± 0.10 |

Notes: Linear and circular polarizations were measured in the V filter except a series of linear polarization data from the literature measured in white light and noted [w]; (★) 1215-002 is classified as a BL Lac by Collinge et al. [2005](#). Sbarufatti et al. [2005](#) re-determined the redshift of 1256-229 ($z=0.481$) and considered this object as a BL Lac. References for linear polarization: (a) Impey & Tapia [1990](#); (b) Berriman et al. [1990](#); (c) Hutsemékers et al. [1998](#); (d) Visvanathan & Wills [1998](#); (e) Schmidt & Hines [1999](#); (f) Lamy & Hutsemékers [2000](#); (g) Sluse et al. [2005](#)

D. Hutsemekers et al.

Table 1. FR II Quasars with Super Eddington Jets

| Source | z | \bar{Q} 10^{45} ergs/s | L_{bol} 10^{45} ergs/s | \bar{R} | freq (10^{15} Hz) | L_{bol}/L_{Edd} | \bar{Q}_{Edd} | ref |
|-------------|-------|-------------------------------|-------------------------------|---------------|-------------------------|-------------------|-----------------|-----|
| 3C 216 | 0.670 | 15.1/14.1 | ≈ 0.12 | ≈ 120 | 0.71/1.16 | 0.05 – 0.1 | 3.3 – 10 | 1 |
| 3C 455 | 0.543 | 7.13/5.04 | 0.38 | 18.7/13.3 | 0.94 | 1.42 | 26.7/18.9 | 2 |
| | | 7.13/5.04 | 0.38 | 18.7/13.3 | 0.94 | 0.07 | 1.33/0.94 | 3 |
| 3C 82 | 2.878 | 155.4/183.8 | 14.5 | 10.7/12.7 | 0.014 | 0.106 | 1.14/1.35 | 4 |
| | | 155.4/183.8 | 25.0 | 6.22/7.35 | 1.67 | 0.245 | 1.52/1.80 | 4 |
| 3C 9 | 2.009 | 148.3/174 | 25.0 | 5.93/6.96 | 1.67 | 0.264 | 1.57/1.85 | 5 |
| | | 148.3/174 | 38.8 | 3.82/4.49 | 0.0078 | 0.324 | 1.24/1.46 | 6 |
| 4C 25.21 | 2.686 | 59.3/59.7 | 11.6 | 5.11/5.15 | 1.14 | 0.198 | 1.02/1.02 | 5 |
| PKS 1018-42 | 1.28 | 63.9/65.2 | 19.3 | 3.31/3.38 | 1.37 | 0.428 | 1.42/1.45 | 7 |
| | | 63.9/65.2 | 14.7 | 4.35/4.45 | 1.37 | 0.326 | 1.42/1.45 | 7 |
| 4C 04.81 | 2.594 | 103.8/148 | 35.8 | 2.90/4.13 | 2.30 | 0.459 | 1.33/1.90 | 5 |
| 3C 196 | 0.871 | 73.5/87.0 | 31.6 | 2.33/2.76 | 1.53 | 3.04 | 7.10/8.41 | 8 |
| | | 73.5/87.0 | 31.6 | 2.33/2.76 | 1.53 | 0.238 | 0.66/0.56 | 9 |
| 3C 14 | 1.469 | 52.38/51.68 | 32.6 | 1.61/1.59 | 1.00 | 0.604 | 1.05/1.03 | 10 |
| 3C 270.1 | 1.519 | 65.1/66.6 | 48.2 | 1.35/1.38 | 2.07 | 0.844 | 1.14/1.17 | 5 |

1. see Punsly (2007), 2. continuum and FWHM from Gelderman and Whittle (1994), M_{bh} from eqn (5), 3. M_{bh} from bulge luminosity estimate in eqn (8), 4. L_{bol} and FWHM raw data from Semenov et al. (2004), M_{bh} from eqn (6), 5. L_{bol} and FWHM from Barthel et al. (1990), M_{bh} from eqn (6), 6. continuum from Meisenheimer et al. (2001), FWHM from Barthel et al. (1990), M_{bh} from eqn(6), 7. Punsly and Tingay (2006), M_{bh} from eqn(7), 8. continuum and FWHM from Lawrence et al. (1996), M_{bh} from eqn (5), 9. continuum and FWHM from Lawrence et al. (1996), M_{bh} from eqn (7), 10. continuum and FWHM from Aars et al. (2005), M_{bh} from eqn (7)

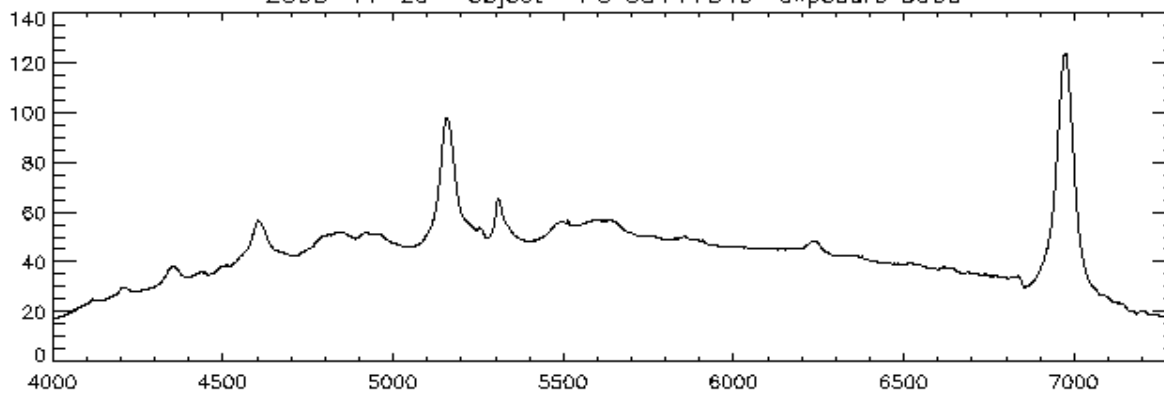
(Brian Punsly, arXiv:0610042v1)

Table 1: Recent Radio continuum observations on globular clusters

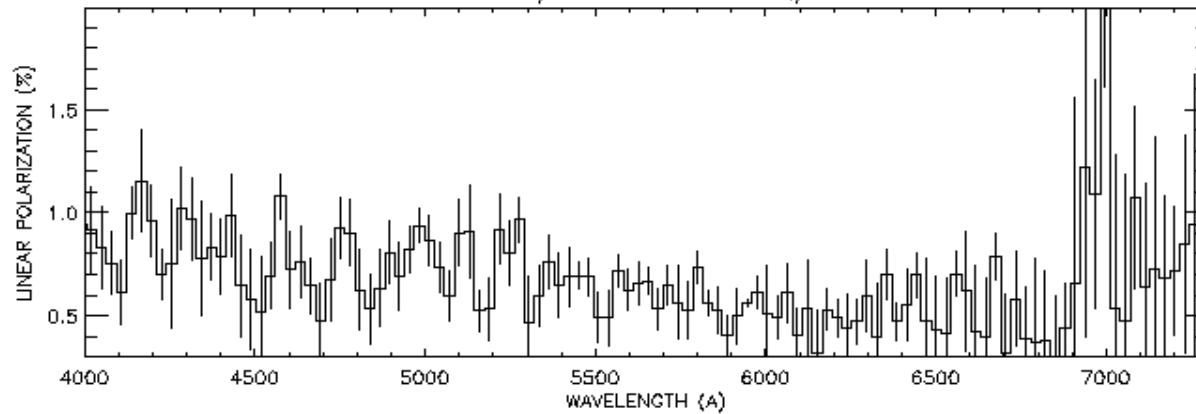
| Cluster name | Distance (kpc) | n_{H} (H cm^{-3}) | T_{gas} (Kelvin) | $F_{\text{R},5\text{GHz}}$ (μJy) | $M_{\text{BH,rad}}$ (M_{\odot}) | $M_{\text{BH,dyn}}$ (M_{\odot}) |
|-----------------|-------------------|--|------------------------------|--|--|--|
| ω Cen | 5.3 | 0.044 | 10^4 | 20 | 5200/1100 | 12000 |
| 47 Tuc | 4.5 | 0.28/0.07 | 10^4 | 40 | 4900/520 | 1500 |
| NGC 6388 | 10.0 | 0.1 | 10^4 | 81 | 1500/735 | 5700 |
| NGC 2808 | 9.5 | 0.26 | 10^4 | 162 | 8500/1800 | 2700 |
| M15 | 10.3 | 0.42/0.2 | 10^4 | 25 | 4900/700 | 1000 |
| M62 | 6.9 | 0.41 | 10^4 | 36 | 2900/600 | 3000 |
| M80 | 10.0 | 0.21 | 10^4 | 36 | 5300/1100 | 1600 |
| NGC 6397 | 2.7 | 0.16 | 10^4 | 216 | 4300/900 | 50 |
| G1 | 780 | ~ 1 | 10^4 | 28 | 4500 | 18000 |

(Ting-Ni Lu, Albert K.H. Kong arXiv:1102.1668v1)

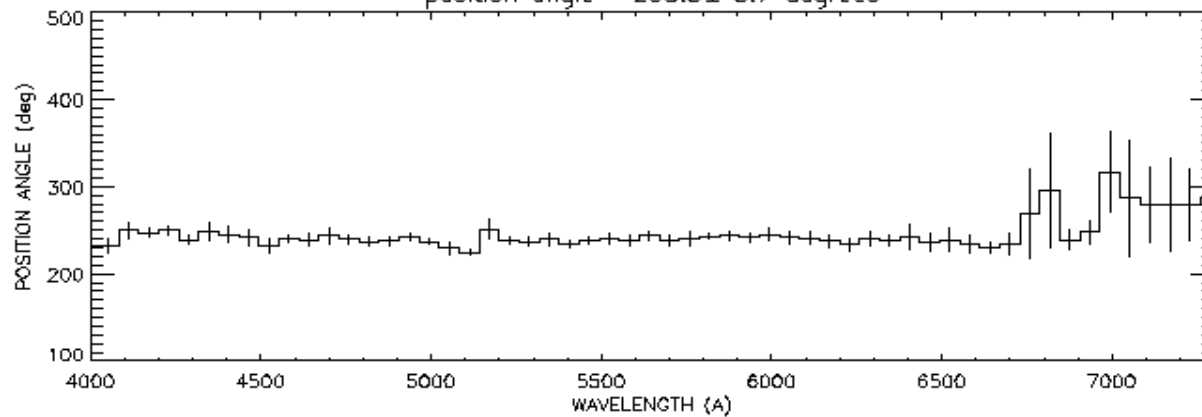
2008-11-29 object PG 0844+349 exposure 3000



$P = 0.66 \pm 0.13\%$ $U/I = 0.67 \pm 0.15\%$ $Q/I = -0.39 \pm 0.17\%$



position angle 238.8 ± 5.7 degrees



QSO B2112+059

Illuminated Disk: $T_e \sim R^{-\frac{1}{2}}$, $a_* = 0.5$

PG 2112+059

$$n = \frac{5}{4}, B(R_\lambda) = 50G, B_H = 4.5 \times 10^3 G, \frac{P_{kin}}{P_{magn}} = 1$$

PG 0026+129

Illuminated Disk: $a_* = 0.5$

$$n = \frac{5}{4}, B(R_\lambda) = 55G, B_H = 2 \times 10^4 G, \frac{P_{kin}}{P_{magn}} = 1$$

PG 0844+349

Illuminated Disk: $a_* = 1$

Ton 951

$$n = 1, B(R_\lambda) = 33.7G, B_H = 1.7 \times 10^4 G, \frac{P_{kin}}{P_{magn}} = 50$$

3C390.3

Illuminated Disk: $a_* = 1$

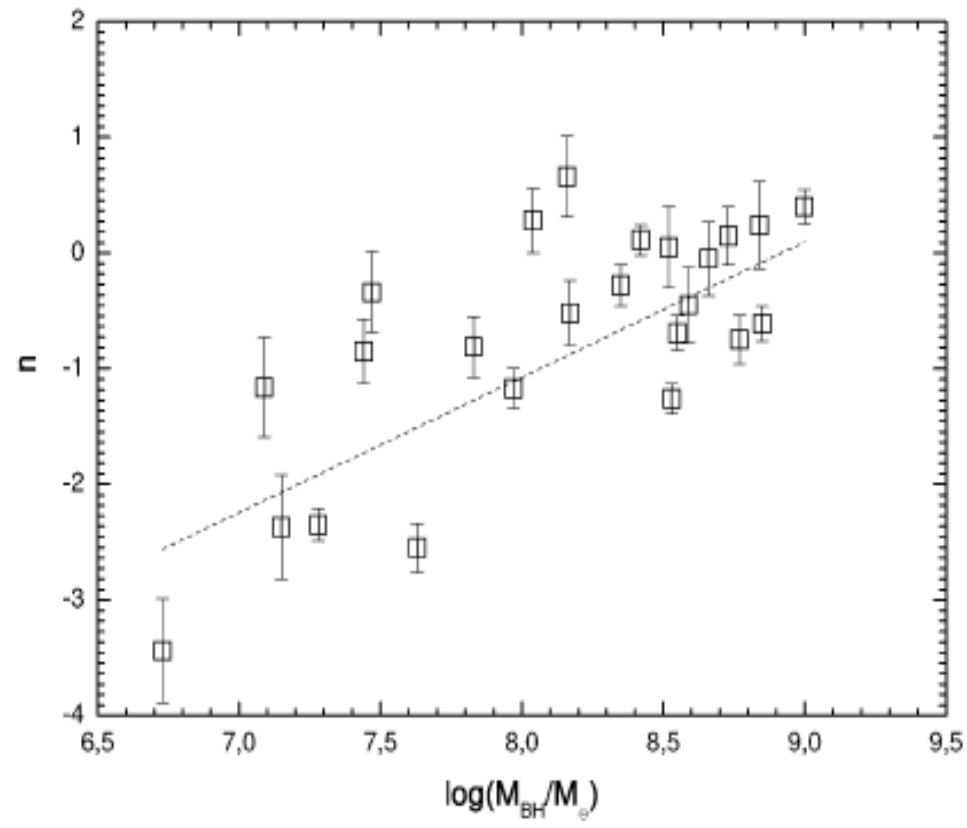
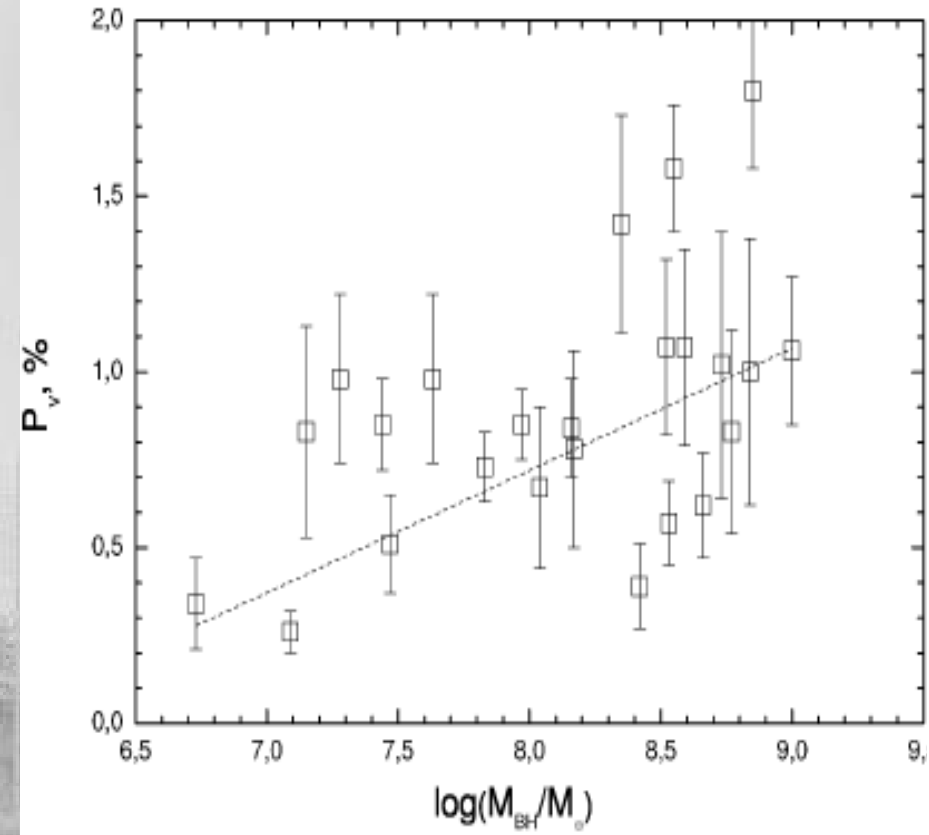
$$n = 1, B(R_\lambda) = 39.3G, B_H = 3.8 \times 10^3 G, \frac{P_{kin}}{P_{magn}} = 10^2$$

Table 2: Masses of the central black holes and polarization in continuum

| Object | Type | $\log \lambda L_\lambda$ [erg/s] (opt.) | $\log \frac{M_{BH}}{M_\odot}$ | Ref. | P_V [%] | n | Ref. |
|-------------|-------|--|-------------------------------|------|-----------------|------------------|------|
| PG 0007+106 | Sy1 | 44.82 | $8.73^{+0.08}_{-0.10}$ | 6 | 1.02 ± 0.38 | 0.15 ± 0.25 | 1 |
| PG 0026+129 | QSO | 45.02 | $8.59^{+0.07}_{-0.12}$ | 7 | 1.07 ± 0.28 | -0.45 ± 0.33 | 1 |
| PG 0049+171 | Sy1.5 | 44.00 | $8.35^{+0.08}_{-0.10}$ | 6 | 1.42 ± 0.31 | -0.28 ± 0.18 | 1 |
| PG 0157+001 | Sy1.5 | 44.98 | $8.17^{+0.08}_{-0.10}$ | 6 | 0.78 ± 0.28 | -0.52 ± 0.28 | 1 |
| PG 0804+761 | QSO | 44.94 | $8.84^{+0.05}_{-0.06}$ | 7 | 1.00 ± 0.38 | 0.24 ± 0.38 | 1 |
| PG 0844+349 | Sy1 | 44.35 | $7.97^{+0.15}_{-0.23}$ | 7 | 0.85 ± 0.10 | -1.17 ± 0.17 | 1 |
| PG 0953+414 | QSO | 45.40 | $8.42^{+0.08}_{-0.10}$ | 6 | 0.39 ± 0.12 | 0.11 ± 0.13 | 1 |
| PG 1022+519 | Sy1 | 43.70 | $7.15^{+0.09}_{-0.11}$ | 6 | 0.83 ± 0.30 | -2.37 ± 0.45 | 1 |
| PG 1116+215 | QSO | 45.40 | $8.53^{+0.08}_{-0.10}$ | 6 | 0.57 ± 0.12 | -1.26 ± 0.13 | 1 |
| PG 2112+059 | QSO | 46.18 | $9.00^{+0.09}_{-0.11}$ | 6 | 1.06 ± 0.21 | 0.40 ± 0.15 | 1 |
| PG 2130+099 | Sy1 | 44.46 | $8.66^{+0.05}_{-0.06}$ | 7 | 0.62 ± 0.15 | -0.05 ± 0.32 | 1 |
| PG 2209+184 | Sy1 | 44.47 | $8.77^{+0.08}_{-0.10}$ | 6 | 0.83 ± 0.29 | -0.75 ± 0.21 | 1 |
| PG 2214+139 | Sy1 | 44.66 | $8.55^{+0.09}_{-0.12}$ | 6 | 1.58 ± 0.18 | -0.69 ± 0.15 | 1 |
| PG 2233+134 | QSO | 45.33 | $8.04^{+0.08}_{-0.10}$ | 6 | 0.67 ± 0.23 | 0.28 ± 0.28 | 1 |
| 3C 390.3 | Sy1 | 43.99 | $8.85^{+0.09}_{-0.11}$ | 6 | 1.80 ± 0.22 | -0.61 ± 0.15 | 1 |
| I Zw 1 | Sy1 | 44.80 | $7.44^{+0.09}_{-0.12}$ | 6 | 0.85 ± 0.13 | -0.85 ± 0.28 | 2 |
| Mrk 509 | Sy1 | 44.28 | $8.16^{+0.04}_{-0.04}$ | 7 | 0.84 ± 0.14 | 0.66 ± 0.35 | 2 |
| Mrk 573 | Sy1 | 44.40 | $7.28^{+0.08}_{-0.10}$ | 8 | 0.98 ± 0.24 | -2.35 ± 0.14 | 3 |
| Mrk 841 | Sy1.5 | 44.29 | $8.52^{+0.08}_{-0.10}$ | 6 | 1.07 ± 0.25 | 0.05 ± 0.35 | 2 |
| NGC 3227 | Sy1.5 | 42.38 | $7.63^{+1.1}_{-1.9}$ | 7 | 0.98 ± 0.24 | -2.55 ± 0.21 | 4,9 |
| NGC 3783 | Sy1 | 43.26 | $7.47^{+0.07}_{-0.09}$ | 7 | 0.51 ± 0.14 | -0.34 ± 0.35 | 2 |
| NGC 4593 | Sy1 | 43.09 | $6.73^{+0.03}_{-0.09}$ | 7 | 0.34 ± 0.13 | -3.44 ± 0.45 | 2,9 |
| NGC 5548 | Sy1 | 43.51 | $7.83^{+0.02}_{-0.02}$ | 7 | 0.73 ± 0.10 | -0.81 ± 0.26 | 5,9 |
| NGC 7469 | Sy1 | 43.72 | $7.09^{+0.05}_{-0.05}$ | 7 | 0.26 ± 0.06 | -1.16 ± 0.43 | 2 |

- (1) This paper; (2) Smith et al. (2002); (3) Nagao et al. (2004); (4) Axon et al. (2008)
(5) Goodrich and Miller (1994); (6) Vestergaard and Peterson (2006); (7) Peterson et al. (2004);
(8) Satyapal et al. (2005); (9) Wu and Han (2001).

(Afanasiev et al. arXiv:1104.3690v1, 2011)



Linear polarization and power-law index n versus black hole masses from the data of Table 2

(Afanasiev et al. arXiv:1104.3690v1, 2011)

| Object | p | s | $B(R_\lambda)[G]$ |
|-------------|-----|-----|-------------------|
| PG 0007+106 | 1/2 | 1 | 2.43 |
| PG 0026+129 | 3/4 | 5/4 | 1 |
| PG 0049+171 | 3/4 | 5/4 | 13 |
| PG 0157+001 | 3/4 | 5/4 | 98 |
| PG 0804+761 | 3/4 | 3/2 | 3.4 |
| PG 0844+349 | 3/4 | 1 | 37 |
| PG 0953+414 | 3/4 | 1 | 300 |
| PG 1116+215 | 3/4 | 3/4 | 100 |
| PG 2112+059 | 3/4 | 2 | 14.4 |
| PG 2130+099 | 1/2 | 1 | 27 |
| PG 2209+184 | 1/2 | 3/4 | 16 |
| PG 2214+139 | 1/2 | 5/4 | 2.8 |
| PG 2233+134 | 3/4 | 3/2 | 0.37 |
| 3C 390.3 | 3/4 | 1 | 6.4 |

Table 3: Physical parameters of the accretion disk obtained from our spectropolarimetric observations at the 6-m BTA telescope (SCORPIO) and published spectroscopic data.

(Afanasiev et al. arXiv:1104.3690v1, 2011)

THANKS FOR ATTENTION!



24.05.2012